

# Effects of the Erosion and Transport of Fine Particles due to Seepage Flow

Donatella Sterpi<sup>1</sup>

**Abstract:** The gradual erosion and transport of fine particles are among the possible consequences to the subsoil of a severe seepage flow, such as the seepage induced by the artificial lowering of the water table by means of pumping wells. The erosion, in turn, could induce local effects, in terms of reductions in the soil volume and variations in the soil mechanical characteristics, that could be non-negligible when working in an urban area. In this paper, some laboratory tests are presented aimed at investigating the erosion of fine particles from soil samples subjected to a controlled seepage flow. The phenomenon of erosion and transport is then modeled by combining, in a single governing equation, the conservation of mass of moving particles with a suitable law of erosion, which is calibrated on the basis of the seepage tests. This equation, coupled with the equation governing the seepage problem, permits one to evaluate the quantity of particles eroded and transported from the soil mass. The effects of the loss of fine material on the stress-strain distribution within the soil mass are estimated by a finite-element analysis. The proposed model is then adopted for the evaluation of the surface settlements induced by the water pumping from a drainage trench.

**DOI:** 10.1061/(ASCE)1532-3641(2003)3:1(111)

**CE Database subject headings:** Erosion; Particles; Seepage; Silty soil; Sand; Drainage.

## Introduction

In the urban area of Milano (northern Italy), a progressive rising of the groundwater table has taken place in the last decades, due to the gradual moving of the relevant industrial plants from the surrounding area and the consequent reduction in water demand from the underlying aquifers.

The water table rising is currently causing serious problems of water inflow within the oldest deep underground structures, such as parking lots and subway tunnels, which were designed, at the time of a low water table level, without a proper waterproof lining. Moreover, the general increase of the pore pressure, and the consequent reduction of the effective stress distribution, might lead to differential settlements of the foundations of major buildings.

Among the solutions currently under investigation, as a possible temporary provision, is the local lowering of the water table by means of pumping wells located in the vicinity of the damaged underground structures. The characteristics of the soil (mainly consisting of silty sand and gravel) and the need to maintain high values of well discharge to attain a constant and sufficiently low level of the water table have drawn attention to the possible erosion of fine particles. As a consequence, the erosion could lead to a local decrease in volume due to the gradual loss of fine material and to the possible rearrangement of the coarser fraction of soil. In addition, the mechanical characteristics of the soil may be af-

ected by the reduction of the fine fraction and by possible changes of the void ratio. These consequences could be of relevance especially when working in an urban area, where they might cause settlements of the foundations of buildings located near the wells.

In literature, the term “erosion” customarily indicates the detachment of a particle from the soil structure, under the mechanical or chemical action of a fluid flow, in the form of surface flow (surface erosion) or internal seepage (internal erosion). In the latter case, the mechanism of macroscopic migration of the detached particle is referred to as particle transport or suffosion (Kovacs 1981; Brauns et al. 1993). The progressive erosion and transport along a flow path may lead to the phenomenon of piping, that is the formation of a large flow channel. Redeposition of a particle occurs due to the presence of a pore constriction along the flow path, that is a pore having a diameter smaller than the particle diameter, or due to the gradual formation of “bridges” among particles. The progressive redeposition of particles can prevent piping by plugging the flow channel.

In literature, the problem of erosion is mainly dealt with in the study of the stability of dams, embankments, and wellbores, in both aspects of surface and internal erosion (e.g., Vaughan and Soares 1982; Sherard et al. 1984a; Stavropoulou et al. 1998). Different, less common, cases can be found where the problem of progressive erosion is reported which leads to differential settlements due to the formation of large voids localized underneath the structures (Hayashi and Shahu 2000).

The internal erosion has been initially investigated with reference to the proper design of dam filters fulfilling the two requirements of preventing soil erosion and piping and allowing for water seepage. Based on experimental investigations (e.g., Sherard et al. 1984b; Kenney et al. 1985), specific filter stability criteria ensuring both requirements have been suggested which prescribe particular conditions on the characteristic diameters of soil and filter grain size distributions (Karpoff 1955; Fischer and Holtz 1996).

<sup>1</sup>Assistant Professor, Dept. of Structural Engineering, Politecnico di Milano, P. Leonardo da Vinci 32, 20133 Milano, Italy. E-mail: sterpi@stru.polimi.it

Note. Discussion open until February 1, 2004. Separate discussions must be submitted for individual papers. To extend the closing date by one month, a written request must be filed with the ASCE Managing Editor. The manuscript for this paper was submitted for review and possible publication on April 27, 2001; approved on May 9, 2002. This paper is part of the *International Journal of Geomechanics*, Vol. 3, No. 1, September 1, 2003. ©ASCE, ISSN 1532-3641/2003/1-111-122/\$18.00.

Together with these geometric characteristics, the influence of other factors on the erosion and transport of particles has been tested as well, such as the hydraulic conditions (fluid velocity and flow direction with respect to the soil-filter interface), the confining pressure, the concentration of moving particles, and the possible chemical reactions (Hadj-Hamou et al. 1990; Reddi et al. 2000; Tomlinson and Vaid 2000).

Besides this experimental research, some attempts have been made to model the phenomenon of particle erosion and transport in a porous medium on the basis of analytical and numerical approaches (Silveira 1965; Wittman 1979; Koenders and Williams 1992; den Adel et al. 1994; Stavropoulou et al. 1998).

The particle detachment can be evaluated on the basis of a limit condition between disturbing forces and frictional/cohesive forces that would prevent the movement (Indraratna and Vafai 1997). If the soil microstructure is seen as a three-dimensional net of channels representing the interconnected voids, along a flow channel, the particle migration is allowed depending either on the probability of meeting a constriction (possible pore clogging) or on the concentration of moving particles (possible flow channel plugging) (Khilar et al. 1985; Atmatzidis 1998). For the evaluation of these situations, geometric conditions should be considered, similar to those involved in the stability criteria for filter design. When the particle migration is possible, flow equations for solid/fluid mixtures can be applied, in which the mass and momentum balance equations play the major role.

In this paper, the problem of erosion and transport of fine particles is addressed with the intent of possible evaluation, based on a numerical modeling, of the induced soil deformations and surface settlements. Toward this purpose, a preliminary laboratory investigation was carried out on samples of silty sand subjected to the flow of water under controlled hydraulic gradients. During these tests, the quantity of eroded particles was measured at different time intervals. The experimental program also included a series of triaxial compression tests carried out on reconstituted samples, having different values of relative density and of fine particle content. The program aimed to evaluate the effects of erosion on the deformability and shear strength of the tested soil.

The seepage tests provided the experimental basis of a law governing the phenomenon of particle erosion from an element of soil. In particular, this law expresses the variation of the quantity of removed particles with time and hydraulic gradient.

The law of erosion, associated with the condition of mass conservation for the particles moving within the soil element, leads to an equation governing the problem at hand. This equation has been implemented in the finite-element analysis of the process of groundwater pumping from a vertical well. The calculations permit one to estimate the development of the surface settlements during time caused by the erosion and transport processes. On these bases, some conclusions are drawn about the potential use of the numerical approach for the analysis of actual field problems.

In the following, specific reference will be made to the framework outlined by Kenney and Lau (1985, 1986) and related definitions. In particular, in their papers, they configure the soil as constituted by a "primary fabric" of fixed particles and an ensemble of loose particles, that can be moved by forces such as those produced by water flow, within the pore network of the primary fabric. The potential transport distance is greater for smaller particles than for larger ones, and it depends on the constriction sizes of the primary fabric pores and on the possible pore clogging due to trapped small particles. The soil has a "stable grading" if its structure is such that the loss of small particles is

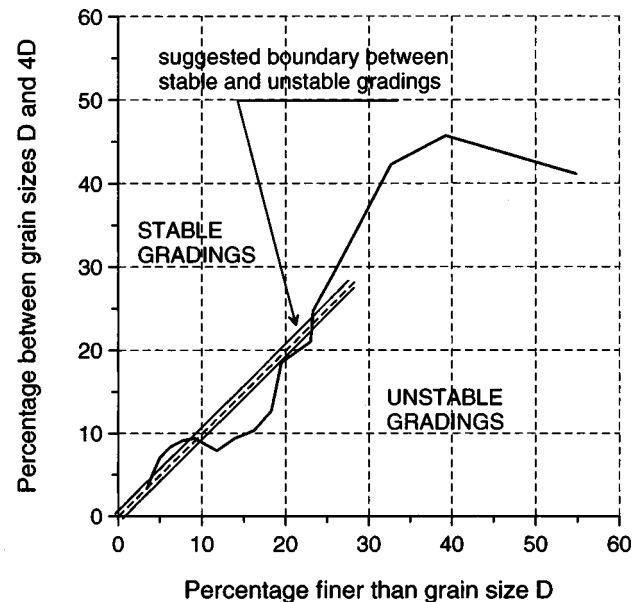


Fig. 1. Shape curve of the soil grain size distribution and boundary between stable and unstable gradings (after Kenney and Lau 1985, 1986)

prevented. In the conclusion, Kenney and Lau suggest a method for predicting the material response based on the analysis of the so-called "shape curve" of the material grading (Fig. 1). This curve is drawn by plotting, for each value of grain size  $D$ , the percentage of mass having grain sizes between  $D$  and  $4D$  versus the percentage of mass having a grain size smaller than  $D$ . A shape curve lying below the suggested boundary line indicates unstable grading. According to this approach, the soil used in the laboratory tests described in the next section has unstable grading (solid line in Fig. 1) and, therefore, could be subjected to erosion.

## Laboratory Tests on Fine Particle Erosion

The soil recovered from borings in the urban area of Milano (Italy) mainly consisted of well graded compacted sand and gravel ( $C_u=38.4$ ,  $G_s=2.72$ ), with a non-negligible percentage of fines (dashed line in Fig. 2). The soil passing through the standard ASTM 200 sieve ( $D=0.074$  mm), in the following re-

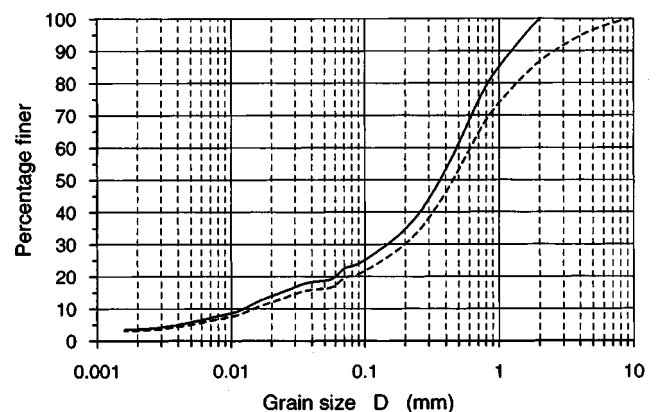


Fig. 2. Grain size distribution for the original soil (dashed line) and for the soil used in the laboratory tests (solid line)

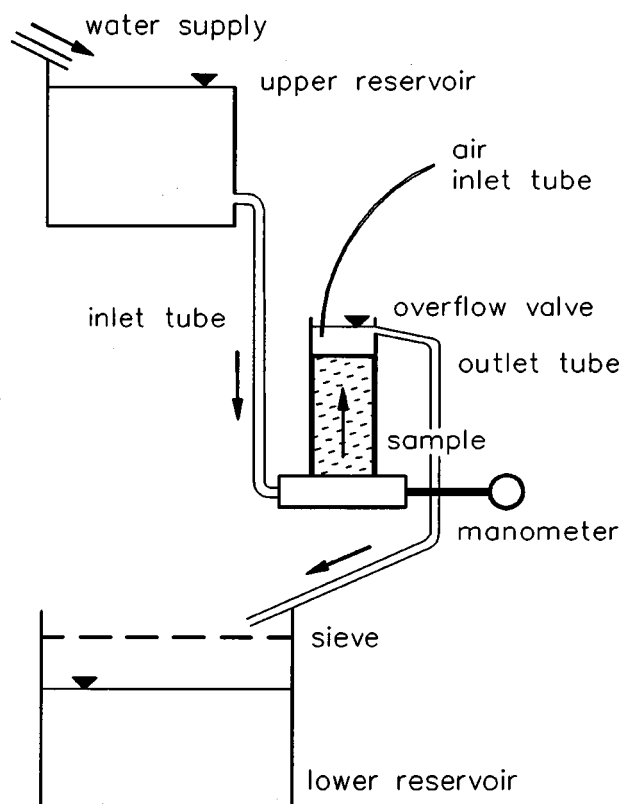


Fig. 3. Experimental setup for seepage tests

ferred to as “fine” material, reached 20% by weight. A relatively high hydraulic conductivity was estimated from *in situ* well pumping tests (average  $k = 10^{-4}$  m/s).

For the laboratory tests, only the material passing through ASTM 10 sieve ( $D = 2$  mm) was considered, due to the relatively small size of the samples. After the gravel component is sifted out, the soil has fines content  $\mu_0$  equal to 23% by weight (solid line in Fig. 2). Maximum and minimum values of void ratio were determined, respectively, by dry pluviation ( $e_{\max} = 0.94$ ) and by standard Proctor compaction tests ( $e_{\min} = 0.33$ ).

To investigate the process of internal erosion of soils, various experimental studies have been proposed in literature that are mainly based on the application of a seepage flow through the soil sample, under a controlled hydraulic gradient, and on the measurement of the amount of removed particles (e.g., Kenney and Lau 1985; Hadj-Hamou et al. 1990). The laboratory tests presented here were based on a similar setup (Fig. 3).

The 14 cm high samples were reconstituted by the moist tamping procedure (Ladd 1978). The quantity of moist soil ensuring an assigned relative density is tamped in seven layers into a membrane held by a vacuum against a cylindrical mold 7 cm in diameter. An initial density of 70% was achieved, corresponding to a void ratio  $e_0$  of 0.51.

The upward seepage flow is induced by the assigned value of the hydraulic head, which depends on the difference in elevation between the upper reservoir and the overflow valve (Fig. 3). The upward direction of the flow was preferred to the downward direction due to the tendency, observed in the preliminary tests, of the fine particles transported by a downward flow to clog the available filtering layer, interposed between the base and the sample itself.

A manometer is connected to the base of the sample to measure the inflow pressure. This allows for the direct evaluation of the hydraulic gradient, thus avoiding possible errors due to hydraulic head losses taking place at the nozzles or within the inlet tube.

A porous stone ensures a uniform flow at the sample base, whereas no filter is placed on the sample head, since it could hinder the removal of particles. The mould is subjected to slight vibrations to prevent the formation of preferential seepage channels. A gentle flow of air is applied at the top of the sample, through a thin tube, to avoid the redeposition of the washed particles on the sample head.

A standard ASTM 200 sieve is placed above the lower reservoir, which collects the water outflow, to separate the fine particles from coarser grains possibly eroded from the soil primary fabric. The amount of coarser grains collected in the sieve was negligible in any case, even for the highest applied gradients.

The lower reservoir is removed and replaced at constant time intervals and the quantity of water is measured. This enables one to evaluate the changes of the soil hydraulic conductivity during the test. The weight of the eroded particles is also measured, after sedimentation and oven drying.

The results of five tests, carried out with various hydraulic gradients, are shown in the diagrams of Fig. 4. They report the increase of the percentage by weight  $\mu_e$  of eroded fine particles with time, for constant hydraulic gradient [Fig. 4(a)], and with hydraulic gradient, for constant elapsed time of seepage [Fig. 4(b)]. The lines in Fig. 4 represent the interpretation of the experimental data through the law that will be discussed in the next section.

The erosion appeared to be rather uniformly distributed within the sample and macroscopic local effects such as preferential flow channels or piping were not noticed. The coefficient of permeability did not change substantially during the tests. Only for the case with a gradient equal to 0.39 was a sudden increase of water outflow observed 5 h after the beginning of the seepage flow, which indicates an appreciable increase of hydraulic conductivity.

The erosion process produces a variation of the soil microstructure and, hence, a possible change of the soil volume or porosity. With respect to this, three alternative hypotheses seem possible on the basis of the relative variations of solid volume  $V_s$  and void volume  $V_v$  induced by the erosion, after the solid volume  $\Delta V_s$  is removed (Fig. 5).

It can be noted that the percentage by volume of eroded particles equals the percentage by weight  $\mu_e$  if the same value of the grain unit weight can be assumed for the fine removable material and for the grains forming the primary fabric. In this case, the variation of the void ratio and the induced volume strains can be easily worked out as functions of the percentage  $\mu_e$ , from the conditions assumed in the three hypotheses:

1. The loss of eroded soil increases the volume of voids without a new arrangement of the primary fabric of the soil [Fig. 5(a)]; in this case, there is the largest increase of the void ratio but the erosion is not associated with volume strains. From the condition of constant total volume ( $V_s + V_v$ ), the following relations are arrived at, for the void ratio  $e$  and the volume strain  $\varepsilon_v$

$$e(\mu_e) = \frac{e_0 + \mu_e}{1 - \mu_e} \quad (1a)$$

$$\varepsilon_v = 0 \quad (1b)$$

An upper limit to the void ratio exists, established by the loosest state that the primary fabric could reach.

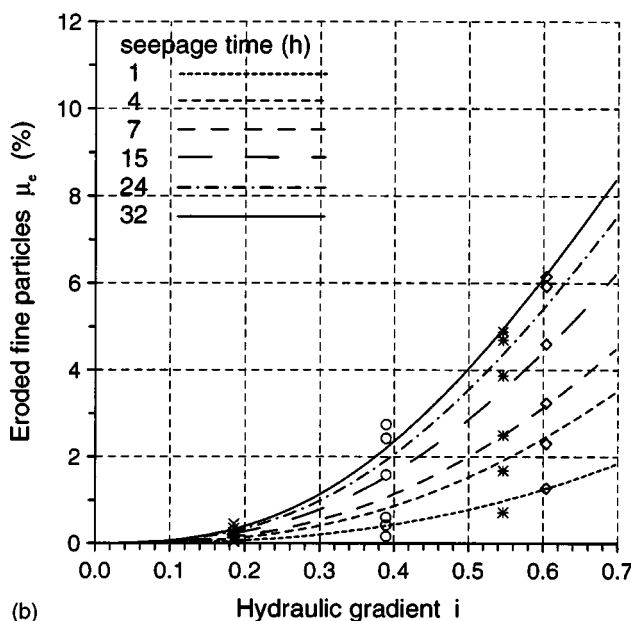
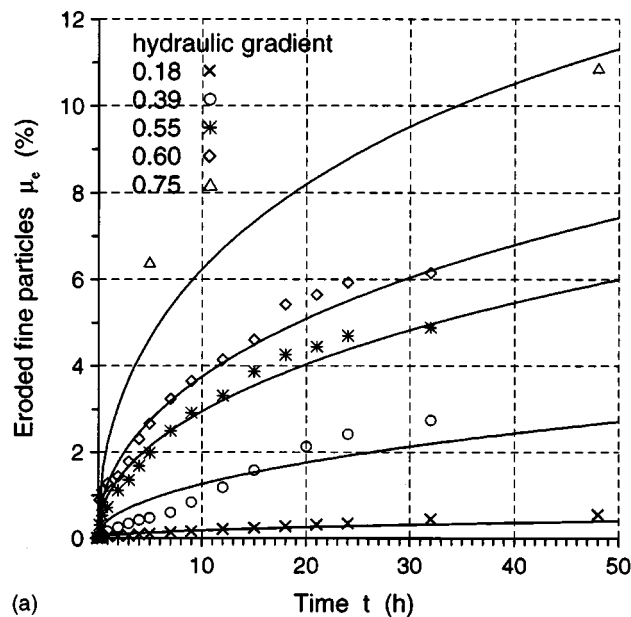


**Fig. 4.** Variations of the percentage by weight of eroded fine particles with time (a) and with hydraulic gradient (b), from laboratory tests (dots) and from their analytical interpretation (solid lines)

- No changes occur in the volume of voids ( $V_V$  is constant) and the total volume reduction is due only to a loss of solid material [Fig. 5(b)]; this causes limited volume strains and a limited increase of void ratio, according to the relations

$$e(\mu_e) = \frac{e_0}{1 - \mu_e} \quad (2a)$$

$$\varepsilon_v(\mu_e) = \frac{\mu_e}{e_0 + 1} \quad (2b)$$

- The total volume reduction is due to the loss of solid material and to an induced compaction of voids [loss of voids indicated as  $\Delta V_V$  in Fig. 5(c)], thus leading to the largest volume strains and to minor variations of the void ratio. An additional hypothesis is necessary in this case to work out

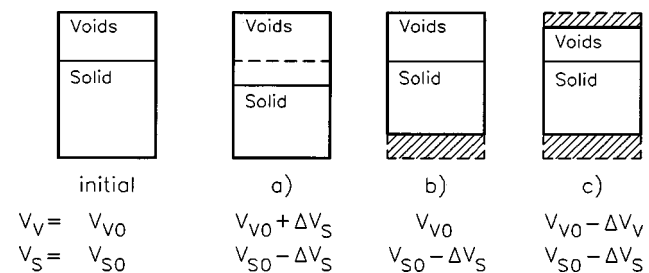


**Fig. 5.** Possible variations of void volume  $V_V$  and solid volume  $V_S$  induced by the erosion process, according to three different cases 1 (a), 2 (b), and 3 (c).

the proper relations. For instance, a zero variation of the void ratio can be assumed, that leads to the condition on the void volume variation

$$\Delta V_V = e_0 \Delta V_S \quad (3)$$

and to the relations

$$e = e_0 \quad (4a)$$

$$\varepsilon_v(\mu_e) = \mu_e \quad (4b)$$

The compaction of voids induced by the erosion process could even lead to a further reduction of the void ratio with respect to the initial value  $e_0$ . The lowest limit to the void ratio is obviously established by the greatest compaction that the primary fabric could permit.

For the soil under consideration, Fig. 6 shows the curves associated with the aforementioned relationships, i.e., the variation of void ratio with respect to the initial value  $e_0 = 0.51$  (solid lines) and the volume strains (dashed lines), with increasing percentage  $\mu_e$  of eroded fine particles.

Further analyses could be made about the variations of relative density induced by the erosion. In this case, it should be considered that the relative density depends, by definition, on the minimum and maximum values of the void ratio for the material at hand, and that these values, in turn, depend on the fines content

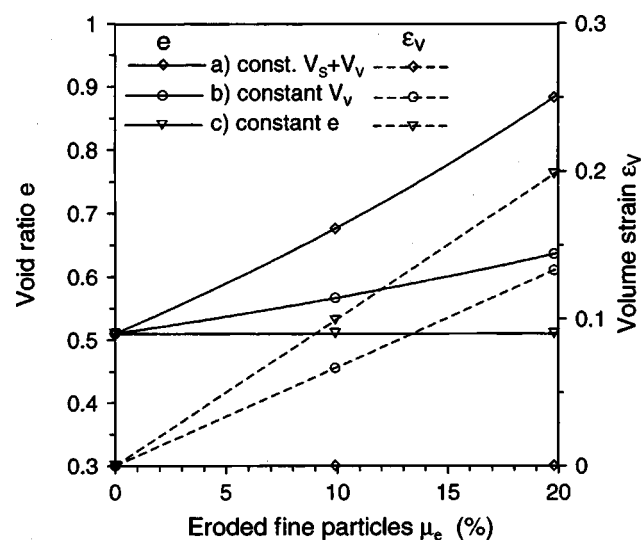


**Fig. 6.** Possible variations of void ratio (solid line) and volume strain (dashed line) with the percentage of eroded fine particles, according to the three cases a, b, and c of Fig. 5

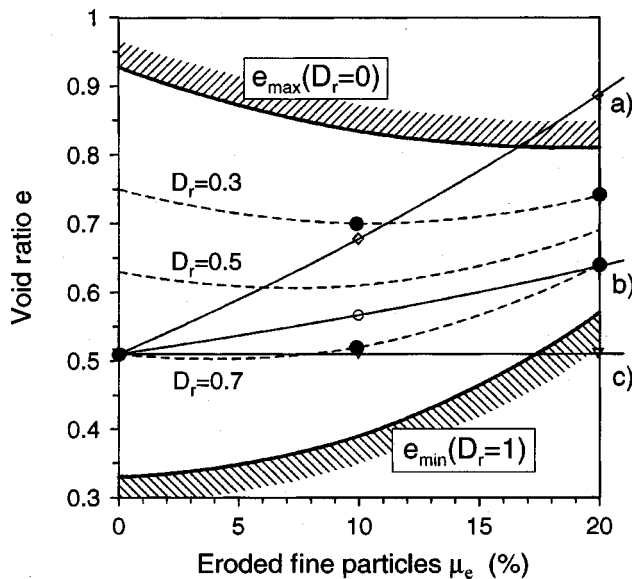


**Fig. 7.** Comparison between the void ratio variations of Fig. 6 and the minimum and maximum void ratio variations, with increasing percentage of eroded fine particles. The dashed lines represent lines at constant relative densities, the dots represent the initial conditions of samples tested in triaxial compression

(Lade et al. 1998; Salgado et al. 2000). Therefore, a preliminary evaluation of  $e_{\min}(\mu_e)$  and  $e_{\max}(\mu_e)$  is required in order to work out the relationship

$$D_r(\mu_e) = \frac{e_{\max}(\mu_e) - e(\mu_e)}{e_{\max}(\mu_e) - e_{\min}(\mu_e)} \quad (5)$$

Fig. 7 reports the same void ratio variations of Fig. 6 in comparison with the variations of minimum and maximum values of  $e$ , experimentally evaluated on samples of the soil under consideration, prepared with various fines contents. The dashed lines of Fig. 7 represent lines at constant relative densities equal to 30%, 50%, and 70%. As expected, together with a possible volume contraction, the erosion process can induce a relevant variation in the soil density (see cases a and c in their opposite tendencies to produce a looser and a denser soil respectively, while case b tends to keep a fairly constant relative density).

At these low values of fines content, less than 25–30%, the mechanical behavior of the silty sand is expected to be dominated by the mechanical behavior of the granular component (Lade and Yamamuro 1997; Thevanayagam and Mohan 2000). However, even minor changes in the fines content or in the soil density could lead to variations of stiffness and shear strength that might be quantitatively relevant.

In order to investigate these variations, a series of drained triaxial compression tests has been carried out on samples prepared without fines content and with a fines content equal to half the original one (Peruzzi 1999). In both cases, the samples were compacted to relative densities of 30 and 70%, representing, for the soil after full or partial erosion, conditions close to those predicted by the described assumptions (see dots in Fig. 7). The results were compared with those obtained from drained triaxial tests carried out on samples of the original soil, prepared at a relative density of 70%, that represents the condition before erosion occurs. Figs. 8(a and b) show the variations of deviatoric

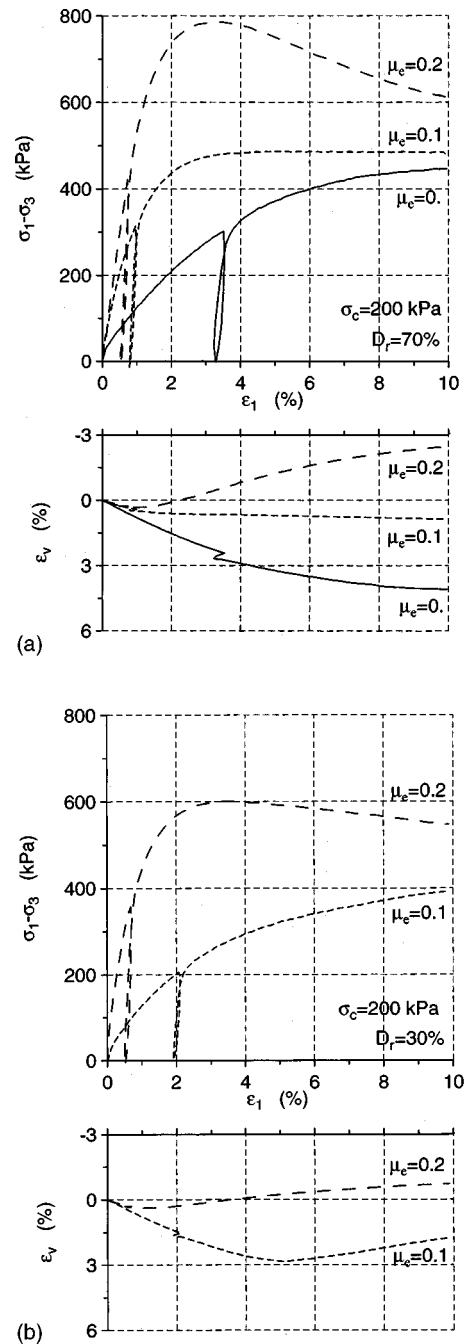


**Fig. 8.** Deviatoric stresses and volumetric strains versus axial strain, from triaxial compression tests on dense (a) and loose (b) samples

stress and volumetric strains with increasing axial strain, for the compression tests carried out with confining effective pressure of 200 kPa.

Table 1 reports the deformability and shear strength parameters estimated from the laboratory tests. For Young's moduli  $E$ , the unloading paths have been considered. The results indicate that the partial or total removal of the fine particles produces, in general, an increase of stiffness and shear strength, for both cases of constant (70%) and reduced (30%) relative densities. Only one case is reported of negligible variation of stiffness and slight loss of shear resistance, that is the case of partial erosion ( $\mu_e = 0.1$ ) associated with a reduction of relative density ( $D_r = 30\%$ ).

**Table 1.** Deformability and Shear Strength Parameters Obtained from Triaxial Compression Tests on the Soil at Hand, at the Initial Condition, and after Partial and Full Erosion

Condition	Percentage $\mu_e$ of eroded fines	Relative density $D_r$ (%)	Young's modulus $E$ (MPa)	Poisson coefficient $\nu$	Friction angle ( $^\circ$ ) (residual–peak)
Initial	0	70	96.76	0.13	32.6
Partial erosion	$\cong 0.1$	70	145.12	0.27	33.2
Partial erosion	$\cong 0.1$	30	96.5	0.13	30.6
Full erosion	$\cong 0.2$	70	172.58	0.31	35.5–41.5
Full erosion	$\cong 0.2$	30	162.2	0.25	34.4–36.9

In addition, other relevant differences among the various tests can be observed that are related to the ductility of the material response and to the dilatant/contractive behavior. In particular, the total loss of fines ( $\mu_e = 0.2$ ) leads to brittleness and dilatancy, especially marked when the erosion occurs without variation of relative density ( $D_r = 70\%$ ). Further investigation on these important issues is currently ongoing.

### Model for Erosion and Transport of Fine Particles

Based on the results of the seepage tests, an empirical law has been derived that describes the process of erosion from the unit volume of soil. The considerable length of the flow path within the sample, compared with the mean grain size, permits one to consider the phenomena of redeposition and pore clogging as already accounted for in the evaluation of the amount of eroded particles from the seepage tests (Khilar et al. 1985; Reddi et al. 2000). In this way, erosion is meant as the effective detachment and transport of the particle. A more rigorous approach would require the separate analyses of the particle detachment (erosion) and particle migration (transport).

For interpreting the laboratory tests, the following relationship is proposed here between the percentage by weight of eroded fine particles  $\mu_e$ , the hydraulic gradient  $i$ , and time  $t$ , expressed in hours

$$\mu_e = \mu_0 \left[ 1 - \exp \left( - \left( \frac{t}{t_0} \right)^b \cdot \frac{i^c}{a} \right) \right] \quad (6)$$

Here,  $\mu_0$  = initial fines content by weight,  $t_0 = 1$  h, and  $a$ ,  $b$ , and  $c$  = nondimensional parameters. These parameters have been backcalculated by minimizing the following function  $E(a, b, c)$ , that represents a measure of the discrepancy between numerical ( $\mu_e$ ) and experimental ( $\mu'_e$ ) results, the former given by Eq. (6)

$$E(a, b, c) = \sum_k [\mu_{e_k}(i, t) - \mu'_{e_k}]^2 \quad (7)$$

The “optimal” solution for the examined samples ( $a = 4.02$ ,  $b = 0.5$ , and  $c = 2.64$ ) led to the lines shown in Figs. 4(a and b).

It has to be pointed out that Eq. (6) has two main consequences. The first one is that erosion occurs for any nonvanishing value of the hydraulic gradient, i.e., no lower limit exists below which the process is absent. In a well graded soil, with fine component in the range of silts, this assumption seems reasonable in view of the fact that even a very low hydraulic gradient could produce erosion of the finest particles. A different behavior might be expected in rather uniform coarse soils, for which a threshold on the hydraulic gradients responsible for erosion can be found (Tomlinson and Vaid 2000).

The second consequence is that, if sufficient time is allowed, there is full erosion, i.e., the erosion process will completely re-

move the fine particles ( $\mu_e \rightarrow \mu_0$  when  $t \rightarrow \infty$ ). However, this second drawback should not be crucial, especially for the engineering problem here considered. In fact, the theoretical time necessary to complete the erosion becomes exceedingly large when the gradient value is within the range met in practical applications. This can be shown, for instance, by plotting the elapsed time  $t_{95}$ , necessary to remove 95% of fine particles versus the hydraulic gradient  $i$  (Fig. 9).

If microscopic mechanisms, such as redeposition and clogging, have already been accounted for, by evaluating  $\mu_e$  from the seepage tests, the transport phenomenon can be related solely to the water flow velocity and direction (den Adel et al. 1994; Indraratna and Vafai 1997).

In the continuous domain of a porous soil subjected to seepage flow, let  $\rho$  and  $\rho_f$  indicate, respectively, the mass density of fine particles and the mass density of nonmoving fine particles in the unit volume of soil. These quantities are functions of the position  $x$ , with reference to a Cartesian three-dimensional coordinate system, and of time  $t$ . Let vector  $v(x, t)$  represent the velocity of the water flow.

In the unit volume of soil, the conservation of mass of fine particles  $\rho$  can be written as

$$\frac{\partial \rho(x, t)}{\partial t} = -\text{div}\{v(x, t) \cdot [\rho - \rho_f](x, t)\} \quad (8)$$

The left-hand side term in Eq. (8) represents the rate of accumu-

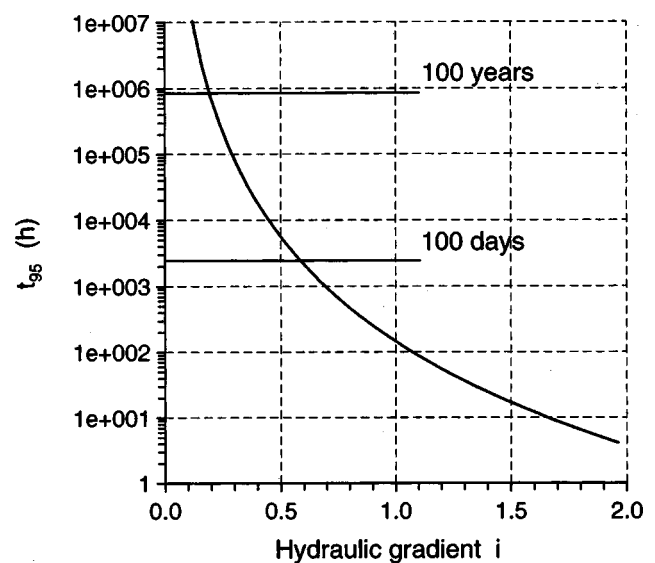


**Fig. 9.** Time span required for the erosion of 95% of fine particles versus hydraulic gradient, according to Eq. (6) with optimum values of parameters  $a = 4.02$ ,  $b = 0.5$ ,  $c = 2.64$

lation of the mass of fine particles, while the right-hand side term is the balance between inflow and outflow masses of moving particles  $[\rho - \rho_f]$ .

The percentage of nonmoving fine particles  $\mu_f$  can be defined as the difference between the initial value  $\mu_0$  and the value  $\mu_e$  of eroded particles

$$\mu_f(\underline{x}, t) = \mu_0(\underline{x}) - \mu_e(\underline{x}, t) \quad (9)$$

On the basis of the law of erosion (6), the following expression for  $\mu_f$  is arrived at:

$$\mu_f(\underline{x}, t) = \mu_0(\underline{x}) \exp \left[ - \left( \frac{t}{t_0} \right)^b \cdot \frac{|\underline{i}|(\underline{x}, t)^c}{a} \right] \quad (10)$$

where parameters  $a$ ,  $b$ ,  $c$  are supposed to be known from a back analysis of experimental data. Note that, in this generic three-dimensional case, the scalar variable  $|\underline{i}|$  represents a suitable measure of the hydraulic gradient in the position  $\underline{x}$  at time  $t$ , equal to the norm of vector  $\underline{i}(\underline{x}, t)$ .

$$|\underline{i}| = \sqrt{\underline{i}^T \cdot \underline{i}} \quad (11)$$

Since the percentages by weight  $\mu$  equal the percentages by mass, the relationship (10) holds also for the density  $\rho_f$  and the initial value of density of fine particles  $\rho_0$

$$\rho_f(\underline{x}, t) = \rho_0(\underline{x}) \exp \left[ - \left( \frac{t}{t_0} \right)^b \cdot \frac{|\underline{i}|(\underline{x}, t)^c}{a} \right] \quad (12)$$

Introducing Darcy's law, that reads

$$\underline{v}(\underline{x}, t) = -\underline{k}(\underline{x}, t) \cdot \underline{i}(\underline{x}, t) \quad (13)$$

the density  $\rho_f$  of Eq. (12) can be expressed as a function of the water velocity  $\underline{v}(\underline{x}, t)$  and of the soil hydraulic conductivity  $\underline{k}(\underline{x}, t)$ . The general form (13) of Darcy's law includes the case of anisotropic characteristics of hydraulic conductivity.

In addition,  $\underline{k}$  in Eq. (13) is considered dependent on the position  $\underline{x}$ , for the case of heterogeneous soils, and on time  $t$ . The latter assumption permits one to consider the possible change in the soil hydraulic conductivity induced by the erosion process. For such a refined analysis, an additional law would be required, calibrated on a suitable experimental investigation and relating the conductivity characteristics to the fines content and to the void ratio or density of the soil at hand. Through this law, an appropriate value could be assigned to parameter  $\underline{k}$ , for any position along each of the assumed paths described in Figs. 6 or 7.

From Eqs. (12) and (13), the rate of erosion can be worked out as a function  $G$  of the water velocity and soil hydraulic conductivity

$$\frac{\partial \rho_f(\underline{x}, t)}{\partial t} = G(\underline{x}, t, \underline{v}, \underline{k}) \quad (14)$$

The governing equation combining the unknown functions  $[\rho - \rho_f]$  and  $\underline{v}$  is finally arrived at by joining Eqs. (8) and (14):

$$\frac{\partial}{\partial t} [\rho - \rho_f](\underline{x}, t) + \text{div} \{ \underline{v}(\underline{x}, t) \cdot [\rho - \rho_f](\underline{x}, t) \} + G(\underline{x}, t, \underline{v}, \underline{k}) = 0 \quad (15)$$

The analysis of boundary value problems, where both the flow velocity  $\underline{v}$  and the density of moving fine particles  $[\rho - \rho_f]$  are unknown, is obtained by coupling Eq. (15) with the equation governing the seepage flow (e.g., Desai 1977). This can be derived by combining Darcy's law (13) with the equation of continuity that governs the flow of an incompressible fluid through a rigid, porous, and saturated medium. The hydraulic head can be

assumed as the unknown variable of the seepage flow problem, the flow velocity  $\underline{v}$  being related to its space derivative, i.e., to the gradient  $\underline{i}$ , through Darcy's law.

Initial and boundary conditions have to be defined for the two coupled problems. Initial values of fine particle density  $\rho_0(\underline{x}, 0)$  and of  $\underline{k}(\underline{x}, 0)$  must be assigned over the whole domain.

On the boundaries, for the seepage analysis, the conditions are assigned, for instance, on the hydraulic head or on its space derivative. In problems with confined flow (i.e., when the seepage takes place in the whole of a geometrically known domain), the conditions should reflect the presence of either pervious or impervious boundaries characterized, respectively, by an assigned value of hydraulic head or by a vanishing value of the component of flow velocity normal to the boundary.

In addition, in the case of unconfined flow, a boundary exists along which the fluid pressure equals the atmospheric pressure, i.e., the condition has to be assigned on the hydraulic head to equal the elevation. Such a boundary can partially coincide with an emerging seepage face, the elevation of which is known, or it can be a phreatic surface, whose geometry is *a priori* unknown. The latter case requires, therefore, an additional condition that, in particular, relates the phreatic surface velocity to the component of the fluid velocity normal to it.

For the problem of erosion and transport, three different kinds of boundaries can be considered. The first is the boundary impervious to both fine particle inflow and outflow. Across it, there is no exchange of moving particles  $[\rho - \rho_f]$ . The second is the boundary, referred to as "negative source," that is considered pervious to one direction only of fine particle transport, that is the particle outflow. Examples of negative sources are the edges of wells and of water reservoirs or the emerging seepage surfaces, that can capture but not produce moving particles. The third case of boundary condition is the one considering the edge as an infinite "positive source," across which particles are captured as well as produced with no limits. More complex situations could be simulated by forcing a negative source to allow a limited absorption of particles. Such a condition could represent the interposition of a filtering layer between the soil and the well or the water reservoir.

Once the proper initial and boundary conditions have been associated with the governing equations, the solution can be obtained in the framework of a suitable numerical method. For instance, in terms of the finite difference method and for the simplest case of a one-dimensional water flow in direction "s," Eq. (15) can be rewritten as

$$(\rho - \rho_f)_{sx}^{t+\Delta t} = (\rho - \rho_f)_{sx}^t - \Delta t \left[ (\rho - \rho_f)_{sx}^t \cdot \frac{v_{sx}^t - v_{s(x-1)}^t}{\Delta x} + v_{sx}^t \frac{(\rho - \rho_f)_{sx}^t - (\rho - \rho_f)_{s(x-1)}^t}{\Delta x} + G(x, t, v_{sx}^t, k_{sx}^t) \right] \quad (16)$$

After the evaluation of the density of moving particles  $[\rho - \rho_f]$ , the total particle density  $\rho$  is then determined, the density  $\rho_f$  being known through Eq. (12).

If the erosion does not appreciably modify the soil hydraulic conductivity, the problems of seepage flow and particle erosion and transport become uncoupled and can be separately solved. In particular, in the case of steady-state flow, a preliminary seepage analysis permits one to evaluate the velocity field  $\underline{v}(\underline{x})$ , constant with time. Then, the step-by-step time integration of the erosion

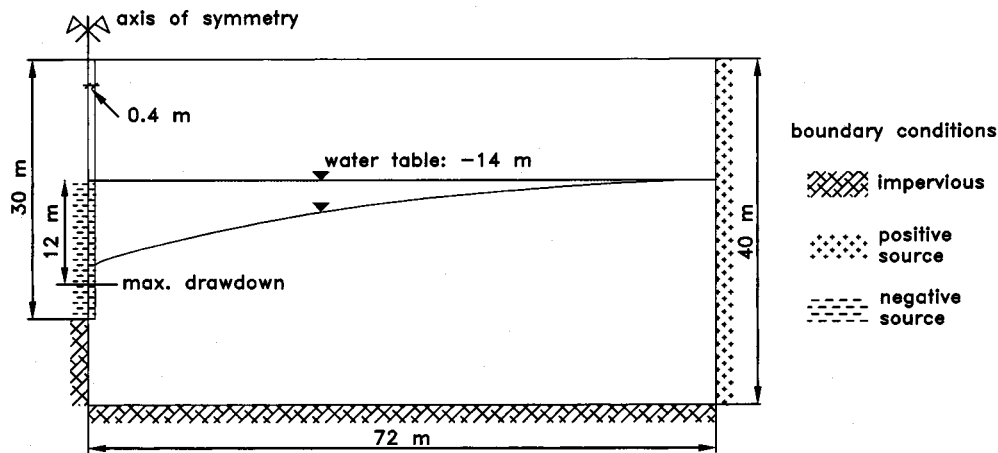


Fig. 10. Geometry and boundary conditions for the drainage trench problem

and transport problem can be based on Eq. (15), where only the function  $[\rho - \rho_f]$  is unknown.

It should be noted, however, that the erosion process begins by definition as soon as the seepage flow begins [cf. Eq. (6)]. Therefore, the steady state is always reached after the transient flow has already induced an erosion of some extent, either in a portion of the domain that belongs also to the domain of the steady-state flow (e.g., in a dam in the case of the reservoir filling) or in a portion that eventually is excluded from that ultimate domain (e.g., for the case of water table lowering). The contribution to the erosion that takes place during the transient phase could be neglected only if the induced void ratio variations and volume strains are distributed over an insignificant portion of the domain, or if the transient phase lasts for a reasonably short time, with respect to the period of time in which the whole process has to be examined.

The case of transient flow would just require a separate evaluation, within each time increment  $(T_i) - (T_{i+1} = T_i + \Delta t)$ , of the velocity field  $\underline{v}(x, T_{i+1})$  and of the consequent density function  $[\rho - \rho_f](x, t)$ .

A preliminary series of finite difference analyses, whose results will not be reported here for brevity (Borelli 2000), has been carried out to validate Eq. (15), in one- and two-dimensional problems with a priori assigned velocity fields and steady-state conditions of seepage.

## Effects on the Soil Mass Strains and Stresses

Once the quantities of eroded and transported particles have been evaluated, a stress analysis is required to estimate the effects of the loss of fine material on the distribution of strains and stresses within the soil mass. Toward this purpose, one of the three assumptions discussed in the section describing the laboratory tests and relating the amount of erosion to the consequent volume strain and the void ratio variation (Fig. 5), should be adopted. Then, from the fine particle density  $\rho$ , evaluated for each time increment over the domain, the induced volume strains (Fig. 6) and the variation of relative density (Fig. 7) are estimated through the chosen relationship. The consequent effects to be considered in the stress analysis are therefore an "initial" strain vector  $\underline{\varepsilon}_0$ , whose entries are related to the induced volume strain, and a variation of stiffness and shear strength characteristics, related to the modified soil density.

If the stress analysis is based on the finite-element method, the nodal force vector  $\underline{f}_0$  equivalent to the initial strains  $\underline{\varepsilon}_0$  is determined according to the following relationship:

$$\underline{f}_0 = \int_V \underline{B}^T \cdot \underline{D} \cdot \underline{\varepsilon}_0 dV \quad (17)$$

where  $\underline{B}$  = matrix of shape function derivatives,  $\underline{D}$  = elastic constitutive matrix and the integral is extended over the element volume  $V$ .

These forces are then applied as external loads and, depending on the problem at hand, the consequent stress/strain changes can be evaluated in an elastic or elastoplastic regime. In the analysis, the modified values of the mechanical parameters can be adopted.

## Application

### Definition of the Geometry and Boundary Conditions

As a first attempt to solve an engineering practice problem, the described solution procedures for the evaluation of the erosion and transport of soil particles and of the consequent effects on the soil mass have been applied to the analysis of the settlements induced by groundwater pumping from a drainage trench (Fig. 10).

The water table is initially located 14 m below the horizontal ground surface. The level of water is then lowered within the vertical trench, 0.8 m wide and 30 m deep, up to -26 m from the ground surface, so that the maximum drawdown reaches 12 m. The soil is assumed to be homogeneous and isotropic, with an initial fines content equal to 20% by weight. The problem was treated under plane strain conditions and, due to its symmetry, only the portion of the soil mass on the right-hand side of the trench was considered in the discretization.

Lateral edges of the domain are constrained in the horizontal component of displacement only. Various horizontal extensions of the soil mass have been considered, from the lowest value of 36 m to the largest of 72 m (cf. Fig. 10), to check the influence of the boundary on the numerical results.

The mesh bottom, located 40 m below the ground surface, is seen as an impervious and rigid boundary the displacements of which are completely constrained. Being impervious to water seepage, the lower boundary is also impervious to particle inflow and outflow.

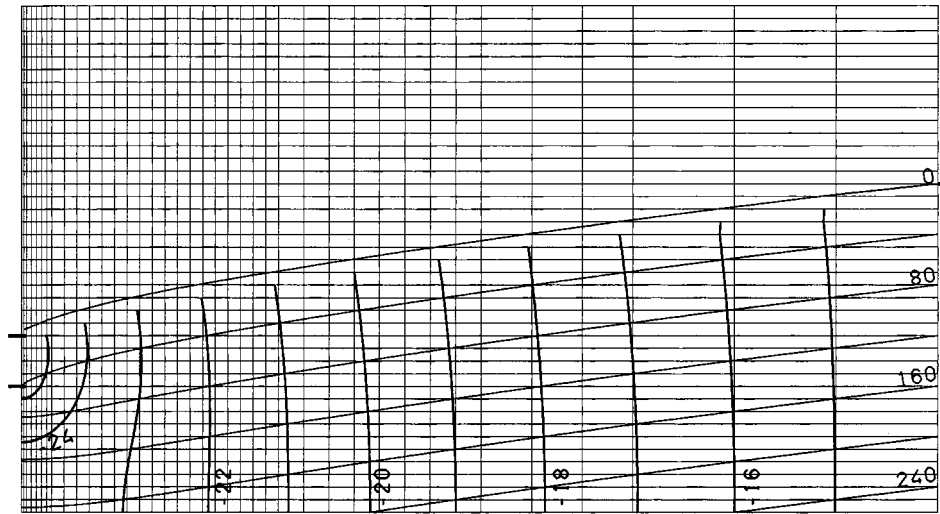


**Fig. 11.** Contour lines of the pore pressure (min=0, max=240 kPa, increment=40 kPa) and of the hydraulic head, in thicker lines (min=15 m, max=25 m, increment=1 m).

Belonging to the axis of symmetry, the portion of the left-hand side boundary below the wall bottom is impervious to water seepage and to particle transport.

On the contrary, the erosion can freely take place through the walls of the trench, where the possible presence of a filter is neglected (negative source assumption), while no change of the initial fines content takes place on the right-hand side vertical boundary (positive source assumption).

The initial stress state depends on the soil unit weight and on the coefficient of earth pressure at rest ( $K_0=0.5$ ). A linear elastic material behavior was assumed in the calculations, since for the problem at hand the stress state induced by the lowering of the water table and by the erosion-transport phenomenon is well within the elastic range. The values assigned to the deformability parameters (Young's modulus  $E$ , Poisson coefficient  $\nu$ ) were obtained from the triaxial compression tests on samples at the condition referred to as initial (cf. Table 1).

### Steady-State, Unconfined Seepage Analysis

Steady-state conditions were assumed for the seepage problem and, neglecting possible changes of the coefficient of hydraulic conductivity, the analyses of seepage and particle erosion were considered uncoupled. Hence, a steady-state unconfined seepage analysis was performed first, resorting to a finite-element approach based on the so-called "fixed mesh" iterative process (Desai 1976; Cividini and Gioda 2000).

This procedure involves a series of analyses on the same finite-element grid, performing an iterative updating of the nodal hydraulic head vector. The series of iterations eventually leads to the solution in terms of position of the phreatic surface and distribution of the hydraulic head, from which the distribution of the flow velocity can be derived.

The first analysis is a confined seepage analysis, carried out on a domain bounded by a trial phreatic surface, located above its likely actual position and considered as an impervious boundary. From the calculated hydraulic head distribution, the values of pore pressure are estimated at each integration point and the distribution of hydraulic conductivity is modified so that points having a negative pore pressure are given a negligible coefficient of

permeability. This new distribution of hydraulic conductivity allows for the evaluation of a sort of residual nodal fluxes, on the basis of which a variation of nodal hydraulic head can be calculated. This variation is then applied in the next iteration, as an updating of the previous values of hydraulic head.

For the analysis on the 72 m large grid, the solution is shown in Fig. 11 in terms of contour lines of the pore pressure and of the hydraulic head. The phreatic surface coincides with the contour line with vanishing pore pressure.

### Analysis of Transient Erosion and Transport of Fine Particles

On the basis of the results of the seepage analysis, in terms of flow velocity distribution, the step-by-step time integration of the erosion-transport problem could be initiated, according to Eq. (15) in which the velocity field  $\underline{v}(\underline{x})$  is considered known and not dependent on time  $t$ .

The analysis was limited to the portion of the domain actually covered by the seepage flow in steady-state conditions. The upper boundary of this new domain is represented by the phreatic surface, which is considered impervious to water seepage and, hence, impervious also to the fine particle inflow and outflow.

The results of calculations are summarized in Figs. 12 and 13, with reference to the analysis on the 36 m large domain. Fig. 12 presents the contour lines of the percentage of nonmoving and total fine particles 1 month after the initiation of water pumping. Note that the quantity of nonmoving particles [Fig. 12(a)] is relatively low in the vicinity of the trench (minimum value=7%). In the same zone, however, the total amount of particles [Fig. 12(b)] is close to its initial value (20%), due to a large quantity of material transported here by the seepage flow. On the contrary, after 12 months, the steady decrease of the quantity of nonmoving particles [minimum value=3% in Fig. 13(a)] is associated with a relevant reduction of the total amount of particles, up to a minimum of 11% [cf. Fig. 13(b)]. A further limited increase of the particle erosion was calculated for considerably larger time intervals beyond 12 months.

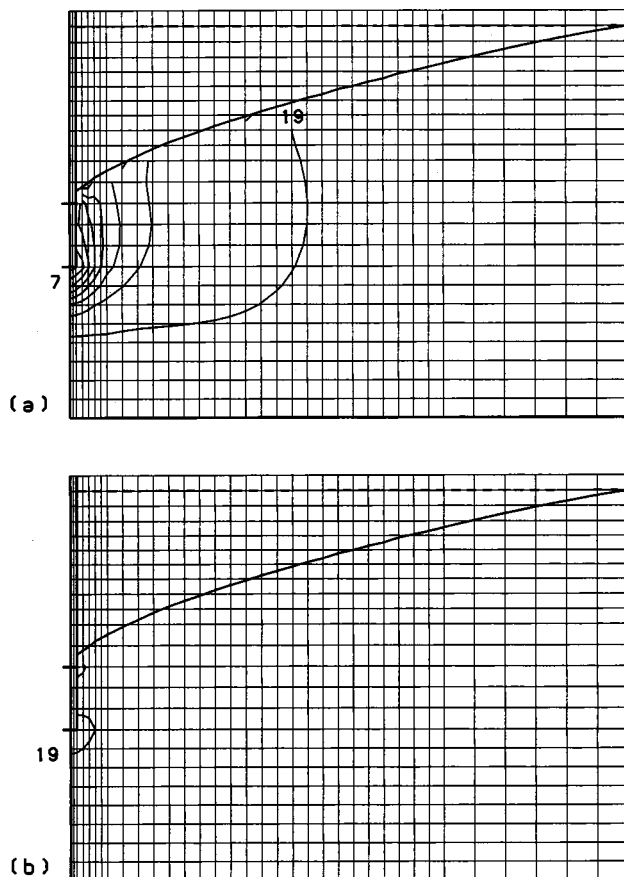


**Fig. 12.** Contour lines of the percentage of (a) nonmoving fine particles  $\rho_f$  (min=7%, max=19%, increment=2%) and (b) total fine particles  $\rho$  (min=19%) after 1 month

### ***Stress–Strain Analysis of the Effects of Water Pumping***

The effects of water pumping on the stress-strain state of the soil mass are shown with specific reference to the surface settlements, which develop at the various stages of the analysis as consequences of different causes. First, the water table lowering causes, by itself, a surface settlement. This is due to the increase of effective stresses occurring when a portion of soil mass turns out to be no longer in the immersed condition. The increase of effective stresses depends on the difference between the natural (or dry) and the buoyant unit weights of the soil and on the extent of the drawdown. In addition, the water flow produces seepage forces that act on the soil particles as the body forces in the direction of flow. These forces are related to the hydraulic gradient distribution and are responsible for surface settlement or heaving depending on the direction of the water flow. The effects of these two contributions were estimated by means of a preliminary stress–strain finite-element analysis carried out in an elastic regime. The dashed line in Fig. 14 summarizes the two effects of seepage and water table lowering in a single curve, representing the nondimensional surface settlements.

Finally, the third contribution to the surface settlements is due to the actual erosion and transport of fine particles. These effects were calculated following the procedure described in the section entitled “Effects on the Soil Mass Strains and Stresses.” In particular, the hypothesis was assumed of constant void ratio and largest volume deformation [case (c) in Figs. 5 and 6], whereas

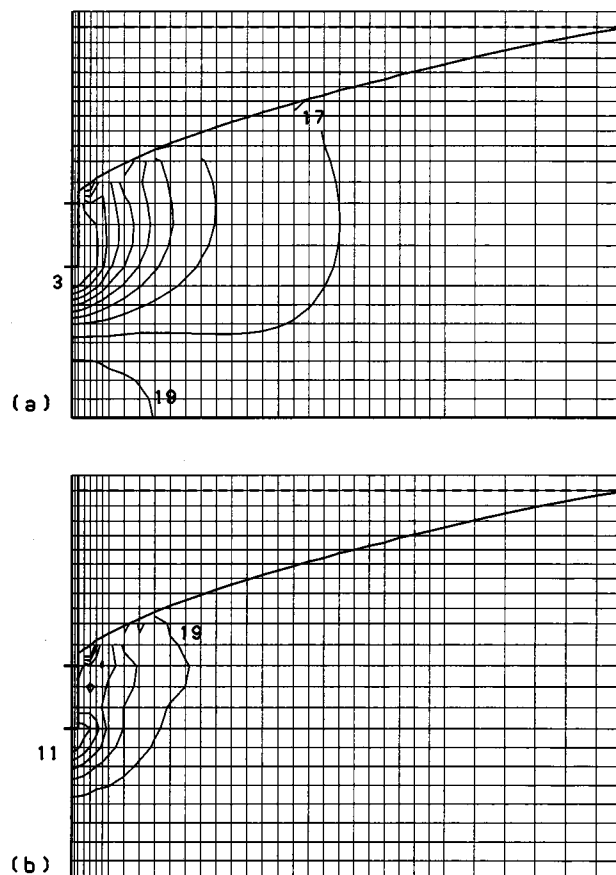


**Fig. 13.** Contour lines of the percentage of (a) nonmoving fine particles  $\rho_f$  (min=3%, max=19%, increment=2%) and (b) total fine particles  $\rho$  (min=11%, max=19%, increment=2%) after 12 months

the increase of soil stiffness, caused by the loss of fine particles (Fig. 8 and Table 1), was neglected. These assumptions are likely to lead to results on the safe side, i.e., to overestimated values of the surface settlements caused by erosion.

The results are shown by solid lines in Fig. 14, with reference to a short- and long-term situation, respectively, 1 and 12 months after the beginning of water pumping. Note that since a very limited increase of erosion was calculated for large time intervals beyond 12 months, the settlement profile attained after 12 months can be considered sufficiently close to the long-term solution profile.

### **Conclusions**

The artificial lowering of the groundwater table by means of pumping wells represents the short-term solution that could be adopted in the urban area of Milano (Italy) for the problem of water inflow of underground structures not properly waterproofed and presently partially submerged by the water table.

In the present study, attention was focused from one side, on the erosion of fine particles from the subsoil as a possible consequence of a severe water seepage and, from the other side, on the effects that the erosion could induce on the existing structures.

A model for the erosion and transport of the fine particles of granular soils, caused by the action of a seepage flow, has been

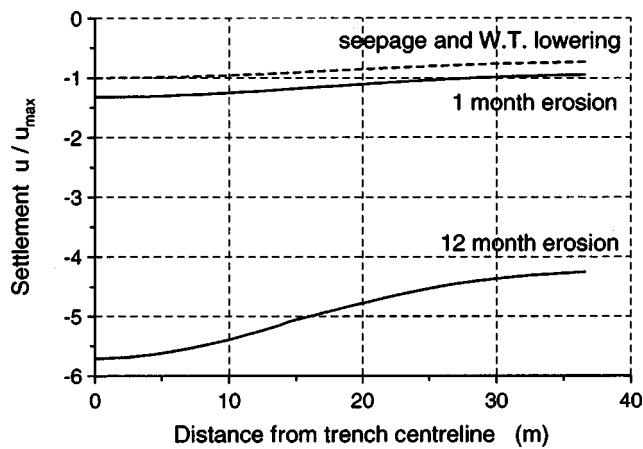


**Fig. 14.** Surface settlements  $u$  due to seepage and water table lowering (dashed line) and due to erosion (solid lines) after 1 and 12 months ( $u_{\max}$  = maximum settlement due to seepage and water table lowering)

discussed. This model is based on an erosion-transport law that has been developed and calibrated considering the results of laboratory seepage tests on reconstituted samples of silty sand. Local volume reductions and variations of the mechanical characteristics have been considered as possible direct consequences of the fine particles erosion.

By coupling the erosion-transport model with a finite-element code for unconfined seepage analysis, and with a stress analysis program, it is possible to estimate the effects induced by the phenomenon of erosion on the soil and surrounding structures. The proposed model has been applied to the analysis of the settlements induced by the water pumping from a drainage trench. The results of the study indicate that some further experimental investigation would be necessary to get better insight into the various aspects of the problem, in particular into those related to the changes in the mechanical properties of the soil subjected to erosion. Besides the variations in stiffness and shear strength, the influence of the fines content on the soil dilatancy and on the postpeak behavior could be investigated as well.

In addition, a refined experimental setup and an extended program of seepage tests could lead to a refinement of the erosion-transport law. An investigation seems necessary, for instance, on the influence of the stress state and of the sample size and on the changes of soil hydraulic conductivity and fluid viscosity during the erosion process.

Although limited by some simplifying assumptions, the numerical approach is promising and it seems worthwhile to extend it toward the analysis of more complex problems. The first step could be an analysis of the same problem here discussed but taking into account the variation in the soil mechanical characteristics associated with the gradual particle erosion. In such a non-linear problem, the coupling of seepage and erosion-transport analyses could be also attempted. A comparison between the approach here discussed and other models for the analysis of erosion and transport of fine particles is currently under consideration.

## Acknowledgments

This study is part of a research program financed by the Metropolitana Milanese S.p.A. (Milan Subway Company). The contri-

butions of S. Borelli and C. Peruzzi and the assistance of E. Iscandri in performing the laboratory tests are gratefully acknowledged.

## Notation

The following symbols are used in this paper:

- $a, b, c$  = nondimensional parameters of Eq. (6);
- $B$  = matrix of shape function derivatives, in the finite-element analysis;
- $C_U$  = uniformity coefficient;
- $D$  = grain size;
- $D_r$  = relative density;
- $\bar{D}$  = elastic constitutive matrix;
- $E$  = Young's modulus;
- $e$  = void ratio;
- $e_{\min}, e_{\max}$  = minimum and maximum void ratios;
- $e_0$  = initial value of void ratio;
- $\underline{f}$  = vector of equivalent nodal forces, in the finite-element analysis;
- $G_S$  = soil specific gravity;
- $k$  = soil hydraulic conductivity;
- $\underline{k}$  = matrix of soil hydraulic conductivity, for two- and three-dimensional analyses;
- $K_0$  = coefficient of earth pressure at rest;
- $i$  = hydraulic gradient;
- $\underline{i}$  = hydraulic gradient vector, for two- and three-dimensional analyses;
- $t$  = time;
- $u$  = surface settlement;
- $u_{\max}$  = maximum surface settlement due to seepage and water table lowering;
- $V_S$  = volume of solids;
- $V_V$  = volume of voids;
- $\Delta V_S$  = volume of solids removed by erosion;
- $\Delta V_V$  = loss of voids induced by erosion;
- $\underline{v}$  = water flow velocity vector;
- $\underline{x}$  = position vector in a Cartesian coordinate system;
- $\underline{\varepsilon}$  = strain vector;
- $\varepsilon_v$  = volume strain;
- $\varepsilon_1$  = axial strain in triaxial compression tests;
- $\mu_e$  = eroded fine particles, percentage by weight;
- $\mu_f$  = nonmoving fine particles, percentage by weight;
- $\mu_0$  = initial fines content, percentage by weight;
- $\nu$  = Poisson coefficient;
- $\rho$  = mass density of fine particles;
- $\rho_f$  = mass density of nonmoving fine particles;
- $\rho_0$  = initial mass density of fine particles;
- $\sigma_c$  = confining cell pressure in triaxial compression tests; and
- $\sigma_1 - \sigma_3$  = deviatoric stress in triaxial compression tests.

## References

- Atmatzidis, D. K. (1989). "A study of sand migration in gravel." *Proc., 12th Int. Conf. on Soil Mechanics and Foundation Engineering*, Rio de Janeiro, Brazil, Balkema, Rotterdam, The Netherlands Vol. 1, 683–686.
- Borelli, S. (2000). "Sull'asportazione di parti fini dal terreno indotta dal pompaggio da pozzo." MS thesis (in Italian), Politecnico di Milano.

- Brauns, J., Heibaum, M., and Schuler, U., eds. (1993). *Proc., 1st Int. Conf. on Filters in Geotechnical and Hydraulic Engineering, Geofilters-92*, Karlsruhe, Germany, Balkema, Rotterdam, The Netherlands.
- Cividini, A., and Gioda, G. (2000). "Finite element analysis of free surface seepage flow," in *Modeling in geomechanics*, M. Zaman, G. Gioda, and J. Booker, eds., Wiley, New York, Chap. 20.
- den Adel, H., Koenders, M. A., and Bakker, K. J. (1994). "The analysis of relaxed criteria for erosion-control filters." *Can. Geotech. J.*, 31, 829–840.
- Desai, C. S. (1976). "Finite element residual schemes for unconfined flow." *Int. J. Numer. Methods Eng.*, 10, 1415–1418.
- Desai, C. S. (1977). "Flow through porous media." *Numerical methods in geotechnical engineering*, C. S. Desai and J. T. Christian, eds., McGraw-Hill, New York.
- Fischer, G. R., and Holtz, R. D. (1996). "A critical review of granular soil filter retention criteria." *Proc., 2nd Int. Conf. on Geofilters*, J. Lafleur and A. L. Rollin, eds., Ecole Polytechnic de Montreal, 409–418.
- Hadj-Hamou, T., Tavassoli, M. R., and Sherman, W. C. (1990). "Laboratory testing of filters and slot sizes for relief wells." *J. Geotech. Eng.*, 116(9), 1325–1346.
- Hayashi, S., and Shahu, J. T. (2000). "Mud pumping problem in tunnels on erosive soil deposits." *Geotechnique*, 50, 393–408.
- Indraratna, B., and Vafai, F. (1997). "Analytical model for particle migration within base soil-filter system." *J. Geotech. Geoenviron. Eng.*, 123(2), 100–109.
- Karpoff, K. P. (1955). "The use of laboratory tests to develop design criteria for protective filters." *Proc., Am. Soc. Testing Mater.*, 55, 1182–1193.
- Kenney, T. C., and Lau, D. (1985). "Internal stability of granular filters." *Can. Geotech. J.*, 22, 215–225.
- Kenney, T. C., and Lau, D. (1986). "Internal stability of granular filters: Reply." *Can. Geotech. J.*, 23, 420–423.
- Kenney, T. C., Chahal, R., Chiu, E., Ofoegbu, G. I., Omenge, G. N., and Ume, C. A. (1985). "Controlling constriction sizes of granular filters." *Can. Geotech. J.*, 22, 32–43.
- Khilar, K. C., Fogler, H. S., and Gray, D. H. (1985). "Model for piping-plugging in earthen structures." *J. Geotech. Eng.*, 111(7), 833–846.
- Koenders, M. A., and Williams, A. F. (1992). "Flow equations of particle fluid mixtures." *Acta Mech.*, 92, 91–116.
- Kovacs, G., *Seepage hydraulics*, Elsevier Science, Amsterdam, 1981.
- Ladd, R. S. (1978). "Preparing test specimen using under compaction." *Geotech. Testing J.*, 1, 16–23.
- Lade, P. V., Liggio, C. D., and Yamamuro, J. A. (1998). "Effects of nonplastic fines on minimum and maximum void ratios of sand." *Geotech. Testing J.*, 21(4), 336–347.
- Lade, P. V., and Yamamuro, J. A. (1997). "Effects of nonplastic fines on static liquefaction of sands." *Can. Geotech. J.*, 34, 918–928.
- Peruzzi, C. (1999). "Avulsione di parti fini dal sottosuolo dovuta al pompaggio da pozzi." MS thesis (in Italian), Politecnico di Milano.
- Reddi, L. N., Lee, I.-M., and Bonala, M. V. S. (2000). "Comparison of internal and surface erosion using flow pump tests on a sand-kaolinite mixture." *Geotech. Testing J.*, 23(1), 116–122.
- Salgado, R., Bandini, P., and Karim, A. (2000). "Shear strength and stiffness of silty sand." *J. Geotech. Geoenviron. Eng.*, 126(5), 451–462.
- Sherard, J. L., Dunnigan, L. P., and Talbot, J. R. (1984a). "Filters for silts and clays." *J. Geotech. Eng.*, 110(6), 701–718.
- Sherard, J. L., Dunnigan, L. P., and Talbot, J. R. (1984b). "Basic properties of sand and gravel filters." *J. Geotech. Eng.*, 110(6), 684–700.
- Silveira, A. (1965). "An analysis of the problem of washing through in protective filter." *Proc., 6th Int. Conf. on Soil Mechanics and Foundation Engineering*, Montreal, University of Toronto, Toronto, Vol. 2, 551–555.
- Stavropoulou, M., Papanastasiou, P., and Vardoulakis, I. (1998). "Coupled wellbore erosion and stability analysis." *Int. J. Numer. Anal. Meth. Geomech.*, 22, 749–769.
- Thevanayagam, S., and Mohan, S. (2000). "Intergranular state variables and stress-strain behavior of silty sands." *Geotechnique*, 50(1), 1–23.
- Tomlinson, S. S., and Vaid, Y. P. (2000). "Seepage forces and confining pressure effects on piping erosion." *Can. Geotech. J.*, 37, 1–13.
- Vaughan, P. R., and Soares, H. F. (1982). "Design of filters for clay cores of dams." *J. Geotech. Eng.*, 108(1), 17–31.
- Wittman, L. (1979). "The process of soil filtration—its physics and approach in engineering practice." *Proc., 7th European Conf. on Soil Mechanics and Foundation Engineering* Brighton, U.K., British Geotechnical Society, London, Vol. 1, 303–310.